Effect of Viscosity Ratio and Processing Conditions on the Morphology of Blends of Liquid Crystalline Polymer and Polypropylene

MARKKU T. HEINO,* PIRJO T. HIETAOJA, TOMMI P. VAINIO, and JUKKA V. SEPPÄLÄ

Helsinki University of Technology, Department of Chemical Engineering, Kemistintie 1, SF-02150 Espoo, Finland

SYNOPSIS

The effect of viscosity ratio and processing conditions on LCP/PP blend morphology was studied. The viscosity ratio (η_{LCP}/η_{PP}) was varied from 0.1 to 3.6 by using five different polypropylene grades as the matrix and two LCPs as the dispersed phase (20 wt %). The most spontaneous fiber formation was achieved when the viscosity ratio was between 0.5 and 1. In addition to shear forces, elongational forces are important in achieving a highly fibrillar structure and significant mechanical reinforcement. The lubricating effect induced by the low viscosity of LCP was most pronounced for the blends exhibiting a fibrillar morphology. The morphologies of blends produced by different mixing equipment differed only slightly. The greatest variation in the mixing efficiency was found for blends whose components had totally dissimilar melt viscosities. The slight differences in morphology due to melt blending in dissimilar equipment were decreased after injection molding, whereas the differences in morphology due to dissimilar viscosity ratios were still evident in the injection molded blends. Thus, the viscosity ratio at processing in the actual processing conditions is of great importance. © 1994 John Wiley & Sons, Inc.

INTRODUCTION

Through blending of thermotropic main-chain liquid crystalline polymers (LCPs) with thermoplastics, the highly oriented fiber structure and good properties of LCPs can be transferred to the more flexible matrix polymer. The usual benefits sought in blending are mechanical reinforcement and improved thermal and dimensional stability achieved through creation of composite-like microstructure. In addition, because of its relatively low melt viscosity a small amount of LCP renders some thermoplastics easier to process.[1-3]

Since the two polymers are immiscible, the blends of LCPs and polypropylene (PP) consist of two separate phases. The dispersed LCP phase exists as small spheres or fibers within the PP matrix and a skin/core morphology is created. The LCP phases are more oriented in the skin region and less oriented in spherical form in the core.

The primary factors determining the size, shape, and distribution of the LCP domains in the matrix are the LCP content, processing conditions, and rheological characteristics of the blend components, in particular the viscosity ratio.[4,5] The morphology is also affected by the interfacial adhesion between the components, which may be modified by the addition of suitable compatibilizers.[6] The effects of shear stress, viscosity ratio, and interfacial tension are related to each other by the Weber number.[7-9] Besides the above, additional drawing greatly enhances the fibrillation and orientation of the LCP phases, resulting in improved strength and stiffness in the fiber direction.[2,4,10]

The effect of viscosity ratio on the morphology of immiscible polymer blends has been studied by several researchers. Min et al.[11] found for polyethylene/polystyrene (PE/PS) blends that when the dispersed phase had a lower viscosity it formed long ligaments in the matrix, but with higher viscosity the dispersed phase was in the form of discrete droplets. Studies with blends of LCPs and thermoplastics have shown similar trends, indicating

* To whom correspondence should be addressed.

Journal of Applied Polymer Science, Vol. 51, 259–270 (1994)
© 1994 John Wiley & Sons, Inc. CCC 0021-8995/94/020259-12

that for good fibrillation to be achieved the viscosity of the dispersed LCP phase should be lower than that of the matrix.[12-15]

The present work consists of two separate but closely related parts. Our overall aim was to carefully study the effects of viscosity ratio (Part I) and blending conditions (Part II) on the morphology of LCP/PP blends. The viscosity ratio was varied between 0.1 and 3.6 by using five different grades of polypropylene and two LCPs.

Since the viscosity of polymers strongly depends on the melt temperature and shear rate, viscosity measurements were made with a capillary rheometer at the blending temperature over a wide range of shear rates. In this way, the blend morphology could be related to the viscosity ratio as it was in the actual processing conditions.

In Part I, extrusion experiments were made with a capillary rheometer and a co-rotating twin-screw extruder. In the former case, the shear rates were measured values, in the latter estimated ones. Attention was paid to the size and shape of the dispersed LCP domains, in particular to the *in situ* fiber formation. The effects of shear and additional drawing are discussed as well.

In Part II, the effect of different mixing equipment and subsequent injection molding on morphology was studied for two blends exhibiting viscosity ratios below and above unity. To allow comparison of the results obtained in Parts I and II, the melt temperatures were kept constant in the extrusion and injection molding experiments and the shear rate ranges were estimated.

EXPERIMENTAL

Materials

The commercial polymers used in the study are characterized in Table I. The polypropylenes PP1–PP5 were supplied by Neste Chemicals, thermotropic liquid crystalline polymer LCP1 by Hoechst Celanese, and LCP2 by Unitika. The polypropylenes were chosen so that viscosity ratios ($p = \eta_{LCP}/\eta_{PP}$) both below and above unity could be obtained. No compatibilizers were added to the blends.

Blending

The blends and blending conditions are presented in Table II. The apparent shear rates in the die were calculated from the equation

Table I Characterization of Materials

Polymer	Melt Index[a] (g/10 min)	T_m (°C)
Matrix		
PP1 = PP VA40 20E	0.4	165
PP2 = PP VB19 50K	1.9	165
PP3 = PP VB65 11B	6.5	165
PP4 = PP VC35 12H	35.0	165
PP5 = PP VC50 76ENA[b]	50.0	165
Minor phase		
LCP1 = Vectra A950	—	280
LCP2 = Rodrun LC-3000	—	220[c]

[a] ASTM D1238 (230°C, 2.16 kg load).
[b] Nucleated.
[c] The lowest recommended processing temperature.

$$\dot{\gamma} = \frac{4\dot{Q}}{\pi R^3} \tag{1}$$

where $\dot{\gamma}$ is apparent shear rate in the die, $\dot{Q}$ the volumetric output of the extruder, and R the radius of the die.[16] The specific energy input (SEI) was calculated from the equation

$$\text{SEI} = \frac{P_{\text{mech}}}{\dot{m}} \tag{2}$$

where P_{mech} is the mechanical power input of the extruder and $\dot{m}$ the output.[17] The extruders used for blending are characterized in Table III. The composition of all blends was 20 wt % of LCP in PP matrix. Prior to blending, LCP1 was dried for 4–5 h at 155°C and LCP2 for 8–10 h at 80°C. The hot extrudates were immediately quenched in a water bath. Samples for the microscopy studies were taken from the extrudates as flown, before pelletizing of the blend for further processing.

Processing

Part I

In addition to viscosity measurements, the capillary rheometer (Göttfert Rheograph 2002) was used to investigate the effect of shear rate on the morphology of the blends prepared earlier in the co-rotating twin-screw extruder (A) with an output of 5.4 kg/h. In these capillary extrusion experiments, the shear rate was varied from 150 to 8000 s^{-1} by adjusting the speed of the piston. The strand was allowed freely to fall into the water bath without extension.

Table II Blending Conditions

Blend	Extruder[a]	Barrel Temperature (°C) T_1	T_2	T_3	T_{die}	Screw Speed (rpm)	Output (kg/h)	Shear Rate in Die[b] (s^{-1})	Specific Energy Input[c] (kWh/kg)
Part I									
LCP1/PP1 (A)	A	275	280	285	285	200	2.4/5.4/8.4	150/350/540	—
LCP1/PP2 (A)	A	275	280	285	285	200	2.4/5.4/8.4	150/350/540	—
LCP1/PP3 (A)	A	275	280	285	285	200	2.4/5.4/8.4	150/350/540	—
LCP1/PP4 (A)	A	275	280	285	285	200	2.4/5.4/8.4	150/350/540	—
LCP1/PP5 (A)	A	275	280	285	285	200	2.4/5.4/8.4	150/350/540	—
LCP2/PP1 (A)	A	220	225	225	225	200	2.4/5.4/8.4	150/350/540	—
LCP2/PP5 (A)	A	220	225	225	225	200	2.4/5.4/8.4	150/350/540	—
Part II									
LCP1/PP1 (A)	A	275	280	285	285	100/300	5.4	350	0.08/0.21
LCP1/PP1 (B)	B	270	290	290	290	45/90	1.7/3.4	55/110	0.07/0.08
LCP1/PP1 (C)	C	285	290	290	290	80/150	6.5	210	0.25/0.29
LCP1/PP4 (A)	A	275	280	285	285	100/300	5.4	350	0.04/0.15
LCP1/PP4 (B)	B	275	280	285	285	45/90	1.4/3.4	50/110	0.04/0.04
LCP1/PP4 (C)	C	Difficulties in blend preparation							

[a] Extruder characterization is presented in Table III.
[b] Calculated from Eq. (1).
[c] Calculated from Eq. (2).

The effect of additional drawing was studied with the LCP1/PP2–3 blends prepared in extruder A with an output of 5.4 kg/h. The additional drawing was done with a Brabender Plasti-Corder PLE 651 laboratory single-screw extruder equipped with a round-hole capillary die (L/D = 55 mm/5 mm) and a belt capstan. All blends were dried before extrusion. The hot extrudate was immediately quenched in a water bath and drawn at various speeds of the takeup machine into strands of different diameter. The draw ratio for each strand was determined as the ratio between the die and strand cross sections (S_0/S_s). The draw ratio ranged from 2 to 13. The melt temperature of these LCP1/PP blends was kept at 290°C and the screw speed was 100 rpm.

Part II

The blends prepared with different mixing equipment were injection molded to test specimens with an Engel ES 200/40 injection molding machine at a melt temperature of 290°C. The shear rate in the nozzle of the injection molding machine was estimated according to Eq. (1) to be about 3000–4000 s^{-1}. Prior to the injection molding the blends were dried for 8 h at 80°C.

Characterization

Part I

Melt rheology of the blend components and blends was characterized by measuring their melt viscosities

Table III Characterization of the Blending Equipment

Extruder	Type	D (mm)	L/D	C_L/D	Screw Configuration
(A) Berstorff ZE 25x33D	Co-rotating twin-screw extruder, closely intermeshing	25	33	0.88	Neutral kneading block at 14D Mixing gears at 18D, 23D, and 28D
(B) Brabender DSK 42/7	Counterrotating twin-screw extruder, closely intermeshing	42	7	0.86	With interrupted flights
(C) Buss-Kneader PR46-11D	Co-Kneader with 3.5D discharge screw	46	11	—	Kneading screw of 11D and discharge screw of 3.5D

in shear flow with a Göttfert Rheograph 2002 capillary viscosimeter. The measuring temperature was 290°C for LCP1 and 230°C for LCP2. The shear rate range from 20 to 10000 s^{-1} was investigated. The L/D ratio for the capillary die was 30 mm/1 mm. Rabinowitch correction was made to the measurements, but Bagley correction was not applied.

The morphology of the fractured surfaces of the extruded and capillary extruded strands was investigated with a JEOL JXA-840A scanning electron microscope (SEM). The samples were fractured at liquid nitrogen temperature in both the flow and transversal directions, and the fractured surfaces were coated with a 15-nm layer of gold.

Some of the extruded and capillary extruded blends were also investigated with an Olympus BH-2 optical microscope equipped with a Linkam HFS91 hot stage. The samples were cut in the flow direction. The fiber formation and dispersion of LCP were studied by melting the PP matrix at 180°C. At this temperature, PP was transparent and the solid, unchanged LCP phase could easily be inspected with transmitted light. This technique appeared to be advantageous in describing the changes in the size and shape of the dispersed LCP phase.

Tensile tests were made on the drawn strands of LCP1/PP2–3(A) with an Instron 4204 tensile testing machine working at a test speed of 3 mm/min.

Part II

The tensile and flexural tests were made on the injection molded blends with an Instron 4204 tensile testing machine equipped with a computer according to ISO R 527 at 23°C. The test speed was 5 mm/min. Before testing the samples were conditioned for 88 h at 23°C (50% RH).

The morphology of the extruded and injection-molded blends was characterized with SEM and the optical microscope as described in Part I.

RESULTS AND DISCUSSION

Rheology

The viscosity behavior of the blend components (PP1–PP5, LCP1 and LCP2) in shear flow is illustrated in Figures 1(a) and 1(b). The corresponding viscosity ratios (η_{LCP}/η_{PP}) are presented in Figures 2(a) and 2(b). In the case of LCP2/PP blends, only the PPs exhibiting the lowest and highest viscosity (PP1 and PP5) were selected for further experiments. The viscosity behavior of LCP1 is more non-Newtonian than that of LCP2, so that different levels of viscosity ratios could be obtained by using two different LCPs. In addition, the shear thinning effect was more pronounced for the polypropylenes. With LCP1 as the minor component, the viscosity ratio ranged from 0.4 to 3.6, while with LCP2 it ranged from 0.1 to 1.5 (150–8000 s^{-1}). Note that the viscosity ratio did not depend only on the polymers used but also on the shear rate.

In extrusion, the shear rate in the die varied from 50 to 540 s^{-1} depending on the output, as estimated by Eq. (1) (Table II). We assumed on the basis of earlier studies[18,19] that under the actual conditions, the shear rate in the screw channel did not exceed 500 s^{-1}. The viscosity ratio in the actual extrusion varied from 0.4 to 2.8 for LCP1/PP (A) blends and from 0.1 to 0.7 for LCP2/PP (A) blends. These ranges were achieved by the use of several different PP grades. In extrusion the viscosity ratio for the individual blends was more or less constant due to the narrow shear rate range. Thus, the differences found in blend morphology could be related to the changes in viscosity ratio. It should be noted that the viscosity ratio is very sensitive to changes in temperature. In this study the temperature was kept constant.

Shear rates are significantly higher in injection molding, and the viscosity ratios of a single blend differ markedly from the values obtained in extrusion as reported in Figure 2. The reader should keep this in mind when the morphology of blends manufactured in different conditions is discussed.

As suggested by earlier reports,[6,14] the addition of LCP decreased the viscosities of the blends. The influence of the viscosity ratio was evident in this lubricating effect, as seen in Figure 3. At the lower shear rate (350 s^{-1}) the greatest viscosity drop, i.e., the difference between the calculated (linear mixing rule) and measured viscosities of the blend was obtained with the smallest viscosity ratio (0.5 for LCP1/PP1). At the higher shear rate (1000 s^{-1}) the viscosity drop was greatest for the blends exhibiting the most fibrillar morphology (LCP1/PP2–PP3). Thus, the highly deformed and oriented LCP phases clearly contributed to the reduction in blend viscosities.

Morphology

Part I: Effect of Viscosity Ratio

Extrusion. The morphology of extruded and capillary extruded nonelongated strands was compared. In extrusion the shear rate in the die was varied by

Fig. 1(a)

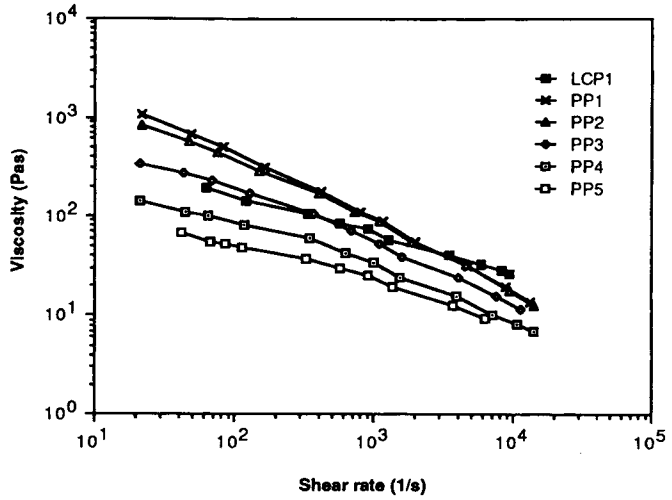

Fig. 1(b)

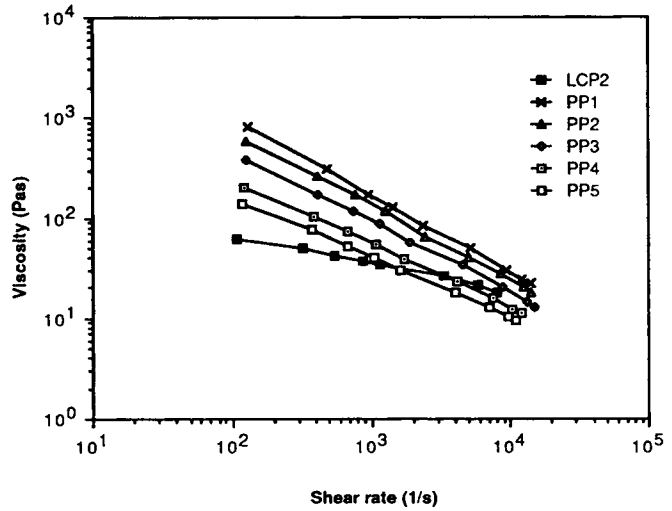

Figure 1 Melt viscosities vs. shear rate for the blend components (a) PP1–PP5 and LCP1 at 290°C and (b) PP1–PP5 and LCP2 at 230°C.

changing the output of the extruder (see Table II). The shear rate in the screw channel was nearly unchanged in all extrusion experiments due to the constant screw speed (200 rpm).

The morphology of the extruded blends was strongly influenced by the viscosity ratio. The most fibrous structure was achieved when the viscosity ratio at extrusion ranged from about 0.5 to 1 [blends LCP1/PP2–PP3 (A)]. In these blends, the dispersion of LCP was smooth and there were a large number of thin elongated fibers. With even lower viscosity ratio [0.4 for blend LCP1/PP1 (A)], a coarser fibrous structure was achieved. By contrast, when the viscosity ratio was increased above unity, the fibrous structure vanished and the LCP domains became spherical or cluster-like. This behavior is illustrated in Figure 4, where the LCP1/PP2 (A) blend represents the most fibrillar structure. With the higher viscosity ratio [2.7 for blend LCP1/PP5 (A)], the LCP domains became clearly spherical.

Capillary Extrusion. The effect of shear on the blend morphology was studied with the nonelongated capillary extruded strands presented in Figure 5. We would again emphasize that the viscosity ratio for each blend changed significantly when the shear rate was increased from 150 to 8000 s^{-1}. Consistent with the results of the extrusion tests discussed above, the three blends in Figure 5 exhibited totally different morphologies. The most fibrillar morphology was achieved with LCP1/PP2 (A) and a slightly coarser fiber structure with LCP1/PP1 (A), while LCP1/

Fig. 2(a)

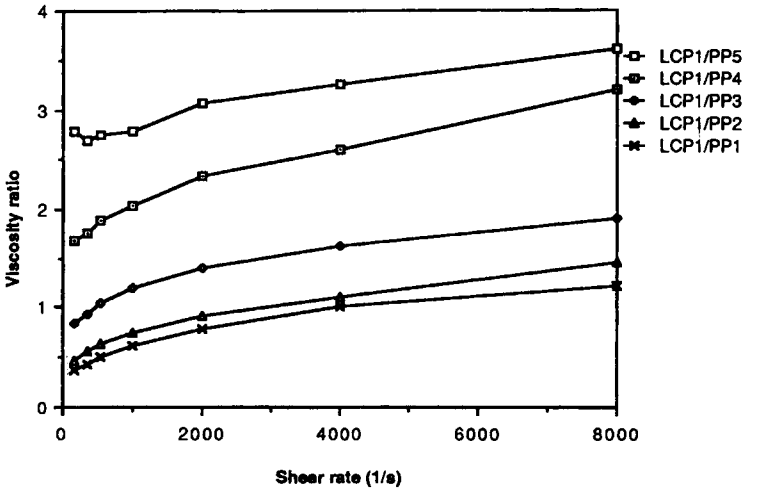

Fig. 2(b)

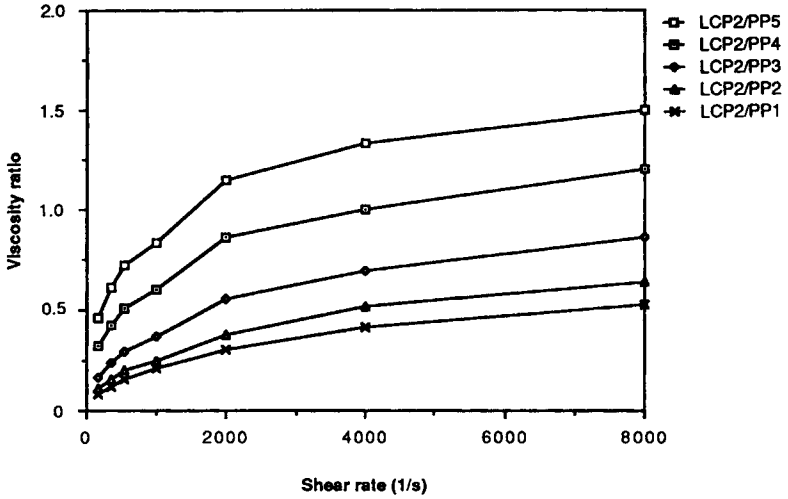

Figure 2 Viscosity ratios vs. shear rate for the blend components (a) LCP1/PP1–PP5 at 290°C and (b) LCP2/PP1–PP5 at 230°C.

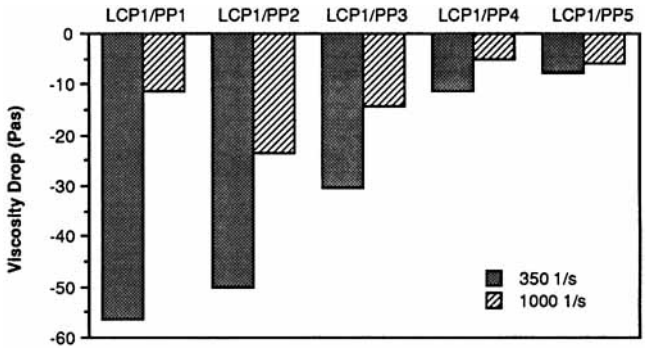

Figure 3 Viscosity drop as the difference between the calculated (linear mixing rule) and measured blend viscosities for LCP1/PP1–PP5 blends at two different shear rates.

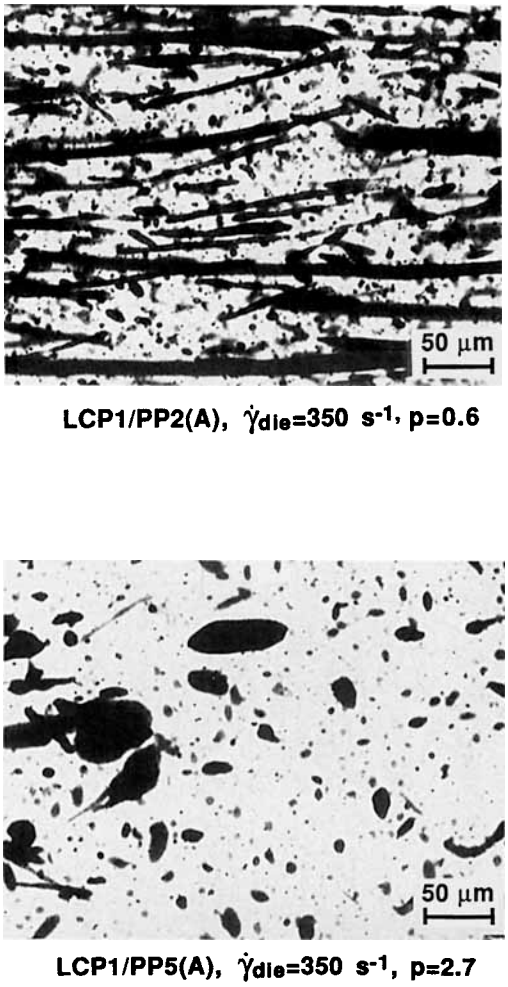

Figure 4 Optical micrographs of the extruded strands in the flow direction of the blends (a) LCP1/PP2 (A) and (b) LCP1/PP5 (A).

PP5 (A) exhibited cluster-like LCP phases and no fibers.

Figure 5 allows the following observations: Increased shear rate did not enhance fiber formation but led to increased coalescence and breaking up of the LCP phases resulting in a nonhomogeneous dispersion. In the case of blends LCP1/PP1–PP2 (A), the increase in shear rate shifted the viscosity ratio to unfavorably high values (from 0.4–0.5 to 1.2–1.5), which are outside the optimal range (0.5–1). However, the increased shear rate did not dramatically change the morphology of any of the blends. Thus, the morphology created during the melt blending stage in the twin-screw extruder was, after all, fairly well maintained in the capillary extruded strands.

Even lower viscosity ratios were obtained with LCP2/PP (A) blends. The morphologies seen in Figure 6 confirm the trends found with LCP1/PP (A) blends. Optimal fiber formation was achieved with viscosity ratios from about 0.5 to 1. When the viscosity ratio decreased to 0.1 [blend LCP2/PP1 (A)], a coarser morphology with fewer fibers was again obtained.

Additional Drawing. The effect of additional drawing on the blend properties and morphology at extrusion was studied with the blends showing most spontaneous fiber formation [LCP1/PP2 (A) and LCP1/PP3 (A)]. As the draw ratio was increased, the elastic modulus and tensile strength of the drawn strands increased significantly, owing to the enhanced fiber formation and orientation. At the draw ratio of 10 the increase in elastic modulus was about 100% and in tensile strength 50%. This is consistent with our earlier studies.[2] Drawing was not applied to blends exhibiting nonfibrillar morphology in the earlier experiments of the study.

Part II: Comparison of Mixing Equipment

Mixing. The blends LCP1/PP1 and LCP1/PP4 were prepared in three different types of mixing equipment, as described in Tables II and III. Note that in extruders A and C the shear rate in the screw channel could be varied without changing the shear rate in the die.

The morphologies of the blend samples LCP1/PP1 (A–C) are shown in Figure 7. Samples were taken in the flow direction from the middle of the extrudate. Blend LCP1/PP1 (C) prepared with the Buss Co-Kneader exhibited the finest dispersion of LCP but without fibers. The same trend was seen in the SEM micrographs of the cross sections of the three blends (Fig. 8). The fine dispersion of LCP1/PP1 (C) might be due to the relatively high values of specific energy input during the blending stage (see Table II). An exceptional morphology was found in blend LCP1/PP1 (B) prepared with the counterrotating twin-screw extruder. Most of the LCP was concentrated in the middle of the strand as a thick, rod-like phase (ca. 1 mm in diameter), evidently due to the poor distributive mixing and channeling of the melt in the extruder and different flow properties of the blend components. The blend LCP1/PP1 (A) prepared in the co-rotating twin-screw extruder exhibited concentric LCP domains, mostly in the form of platelets.

In LCP1/PP4 (A–B) blends the LCP did not form fibers but exhibited a dispersion of spherical LCP domains.

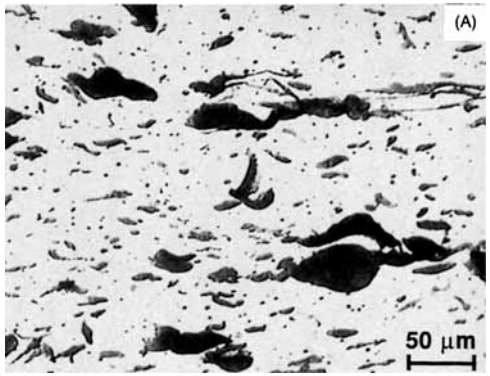

LCP1/PP1(A), $\dot{\gamma}_{die}$=8000 s^{-1}, p=1.2

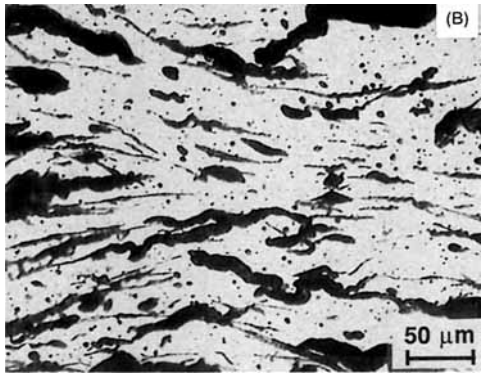

LCP1/PP2(A), $\dot{\gamma}_{die}$=8000 s^{-1}, p=1.5

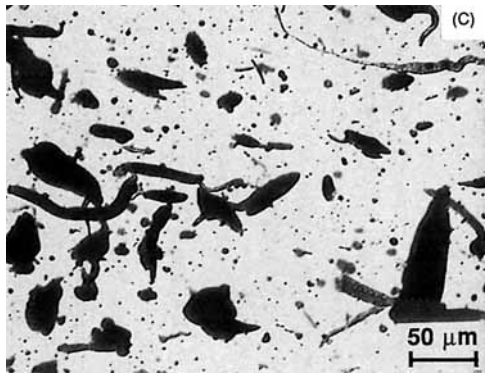

LCP1/PP5(A), $\dot{\gamma}_{die}$=8000 s^{-1}, p=3.6

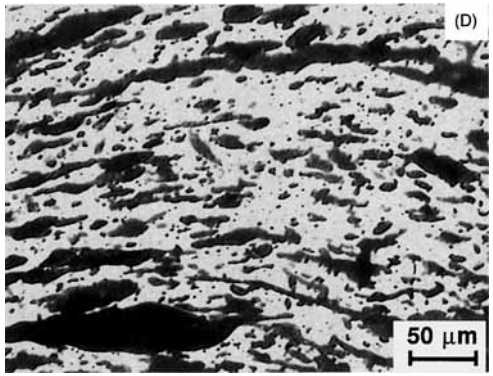

LCP1/PP1(A), $\dot{\gamma}_{die}$=150 s^{-1}, p=0.4

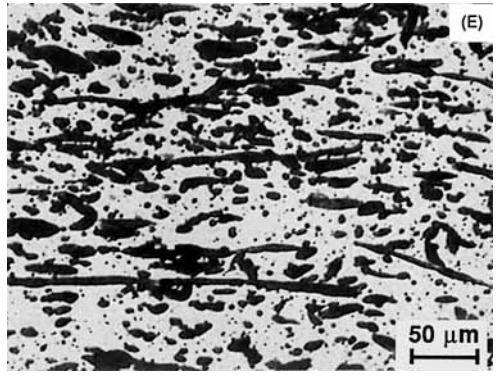

LCP1/PP2(A), $\dot{\gamma}_{die}$=150 s^{-1}, p=0.5

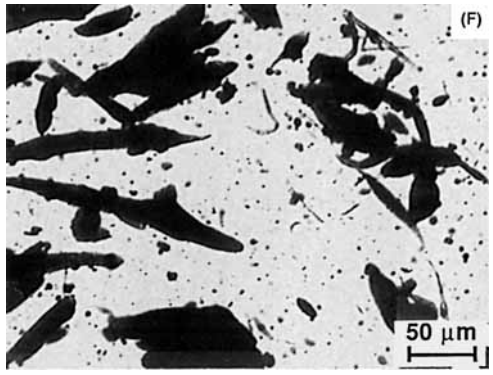

LCP1/PP5(A), $\dot{\gamma}_{die}$=150 s^{-1}, p=2.8

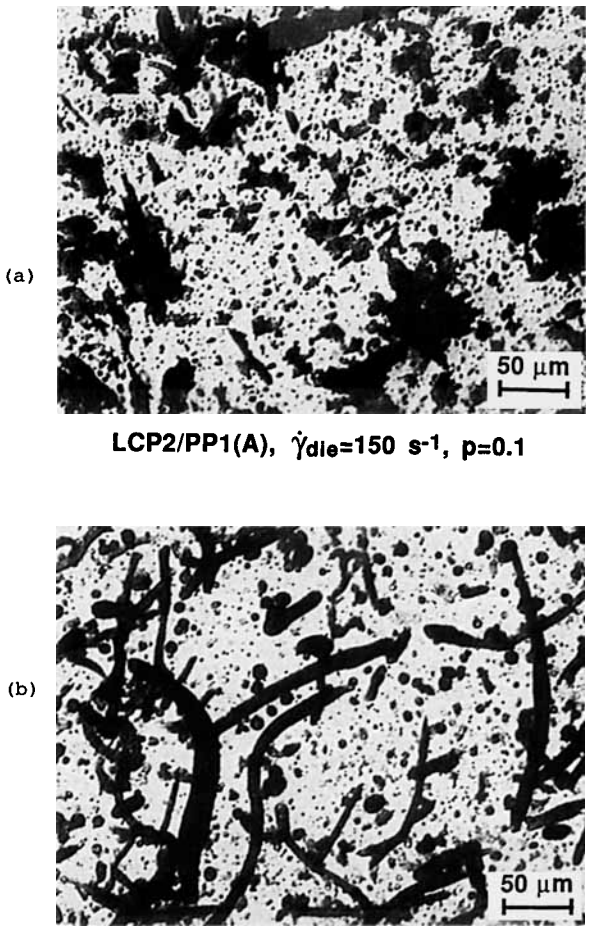

Figure 6 Optical micrographs of the capillary extruded strands in the flow direction at $\dot{\gamma}_{die}$ = 150 s^{-1} of the blends (a) LCP2/PP1 (A) and (b) LCP2/PP5 (A).

The variation in screw speed of the extruder (Table II) appeared to have a negligible effect on the blend morphology.

Injection Molding. The morphology of the injection-molded blends is shown in Figure 9. The samples were cut from the core of the molded specimen to obtain comparable micrographs and avoid the disturbing effect of the highly deformed skin layer. The morphology created by the twin-screw extruders (A, B) in the blending stage was fairly well maintained after the injection molding, as seen in Figures 7 and 9. Exceptionally, the thick rod-like core of the blend

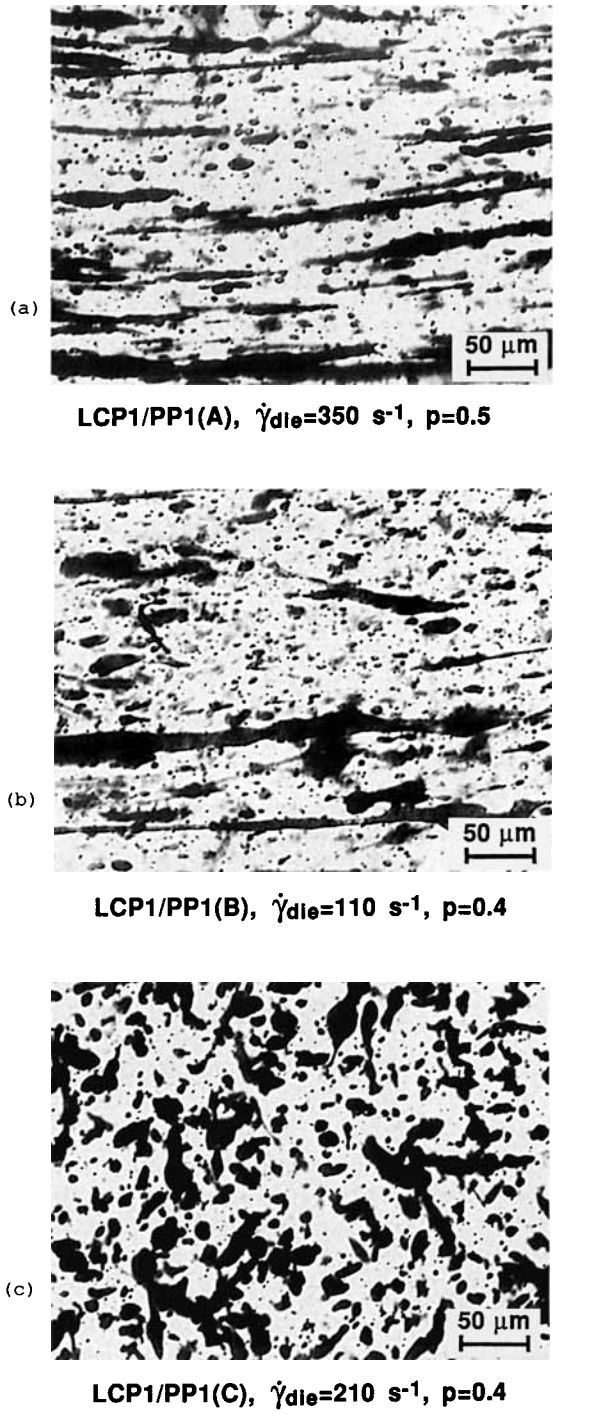

Figure 7 Optical micrographs of the extruded strands in the flow direction of LCP1/PP1 blends prepared with (a) extruder A at 300 rpm, (b) extruder B at 90 rpm, and (c) extruder C at 150 rpm.

Figure 5 Optical micrographs of the capillary extruded strands in the flow direction at $\dot{\gamma}_{die}$ = 8000 s^{-1} of the blends (a) LCP1/PP1 (A), (b) LCP1/PP2 (A), and (c) LCP1/PP5 (A), and at $\dot{\gamma}_{die}$ = 150 s^{-1} of the blends (d) LCP1/PP1 (A), (e) LCP1/PP2 (A), and (f) LCP1/PP5 (A).

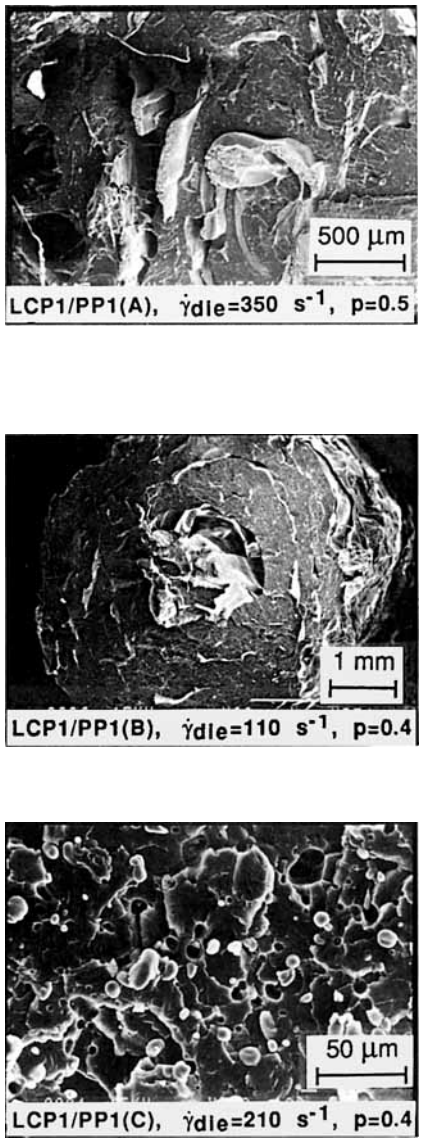

Figure 8 SEM micrographs of the cross sections of the extruded strands of LCP1/PP1 blends prepared with (a) extruder A at 300 rpm, (b) extruder B at 90 rpm, and (c) extruder C at 150 rpm.

LCP1/PP1 (B) was no longer present in the injection-molded specimens. The morphology of the blend LCP1/PP1 (C) prepared with the Buss Co-Kneader became more like that of the two other blends, LCP1/PP1 (A) and LCP1/PP1 (B), after injection molding. This observation confirms our earlier finding that, for an individual blend, the morphology of the injection-molded specimen is not strongly dependent on the melt blending stage.[6] Thus, for LCP1/PP4 (A–B) blends the injection-molded and extruded samples were not significantly different.

The mechanical properties of injection-molded blends with similar composition but different blending history were about the same. Nevertheless, the injection-molded LCP1/PP1 blend showed better strength and stiffness than the LCP1/PP4 blend independently of the mixing equipment. Evidently this was due to the nonfibrous structure of the

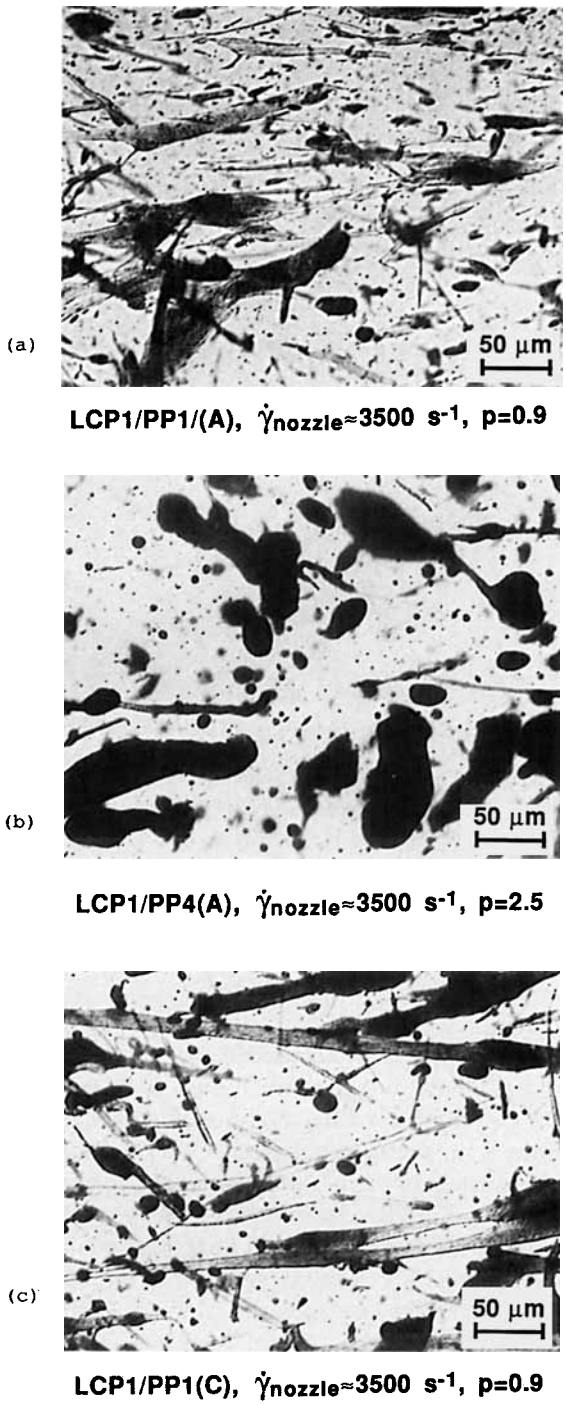

Figure 9 Optical micrographs of the injection-molded test specimens in the flow direction of blends (a) LCP1/PP1 (A, 300 rpm), (b) LCP1/PP4 (A, 300 rpm), and (c) LCP1/PP1 (C, 150 rpm).

LCP1/PP4 (A–B) blends. Among the injection-molded specimens, the LCP1/PP1 blend exhibited a clear skin/core morphology with more oriented LCP fibers in the skin region, whereas the LCP1/PP4 blend, which had an unfavorably high viscosity ratio, had no skin region at all. The viscosity ratio was thus an important factor in determining the morphology of the injection-molded blends.

The morphologies of the injection-molded samples are consistent with the capillary extrusion results reported in Part I.

Interfacial and Rheological Effects

The basic principle of droplet deformation is that if the viscous forces exceed the cohesive forces of surface tension, the droplet will break up. Prior to the break-up the droplet deforms to a cylindrical elongated form. The deformation and break-up conditions for Newtonian liquids can be estimated by the Weber number (We) obtained from the equation

$$\mathrm{We} = \frac{\eta_m \dot{\gamma} r}{\gamma_{12}} \tag{3}$$

where η_m is the viscosity of the matrix, $\dot{\gamma}$ the shear rate, r the radius of the droplet, and γ_{12} the interfacial tension.[7,8] For a viscoelastic drop, on the other hand, the critical condition for droplet break-up is

$$\mathrm{We} \geq \frac{F(p)}{\sin(2\phi)} \tag{4}$$

where $F(p)/\sin(2\phi)$ is an empirical function of the viscosity ratio p, orientation angle ϕ, and some elastic parameters of the system.[9] According to Wu,[9] the critical Weber number is

$$\mathrm{We}_{cr} = 4p^{\pm 0.84} \tag{5}$$

Table IV Calculated Particle Sizes of the Dispersed LCP Phase According to Eqs. (3) and (5)

Blend	Fig.	$\dot{\gamma}$ (s^{-1})	η_m (Pa)	p	$r_{calc.}$ (μm)
LCP1/PP1 (A)	5 (a)	8000	24	1.2	0.14
LCP1/PP2 (A)	5 (b)	8000	20	1.5	0.20
LCP1/PP5 (A)	5 (c)	8000	8	3.6	1.04
LCP1/PP1 (A)	5 (d)	150	340	0.4	0.95
LCP1/PP2 (A)	5 (e)	150	270	0.5	1.00
LCP1/PP5 (A)	5 (f)	150	45	2.8	7.90

Interfacial tension for LCP1/PP blend $\gamma_{LCP1/PP}$ = 11.4 mN/m at 290°C.[19,20]

where the exponent is positive when $p > 1$ and negative when $p < 1$.[9]

Since the average particle sizes were difficult to measure from the micrographs, they were calculated for the LCP1/PP blends according to Wu's theory as reported in Table IV. The interfacial tension needed for the calculations was estimated according to Wu by using the harmonic mean equation.[20] The surface tension for LCP1 needed for this calculation was that measured by Heidemeyer.[19] The trend in particle size seen in the micrographs—larger particles at higher viscosity ratios—was in agreement with theory. However, the measured particle sizes were significantly larger than the calculated ones. The difference may be due to the unknown parameters in Eq. (4). For example, the elastic properties of the blend components may have a crucial effect on the droplet deformation and break-up.

CONCLUSIONS

Study of the effect of viscosity ratio on the morphology of LCP/PP blends showed the most fibrous structure to be achieved when the viscosity ratio (η_{LCP}/η_{PP}) ranged from about 0.5 to 1. At even lower viscosity ratio the fiber structure was coarser, while at viscosity ratios above unity, the LCP domains tended to be spherical or cluster-like.

In all experiments the measured viscosities of the blends were lower than those calculated by the linear mixing rule. At lower shear rates ($< 350\ s^{-1}$), LCP1/PP blends with the lowest viscosity ratio ($p = 0.5$) showed the greatest viscosity drop, whereas at higher shear rates ($> 1000\ s^{-1}$) it was the blends with most fibrillar structure that exhibited the most pronounced viscosity drop. Thus, also the lubricating effect induced by the LCP was greatest when the viscosity ratio was below unity.

Increased shear rate caused slight changes in the blend morphology but did not enhance the fiber formation. Thus, in addition to shear, elongational forces are needed to achieve a well-fibrillated blend structure and significant mechanical reinforcement.

Blends prepared in different mixing equipment showed some slight differences in blend morphology. The blends prepared with the Buss Co-Kneader-type extruder exhibited the finest dispersion of LCP phases. In contrast, the channeling effect and phase separation were most pronounced for the counter-rotating twin-screw extruder, in particular, for blends whose components had totally different melt viscosities.

The slightly different morphologies after melt blending in different equipment were less pro-

nounced after injection molding. We would emphasize, however, that the dissimilarities in morphology attributed to dissimilar viscosity ratios were systemically carried over to the injection-molded blends.

In manufacturing and processing polymer blends, it is important that the viscosity ratio be within the optimal range in the actual processing conditions. Thus, not only the polymers to be blended but also the temperature and shearing conditions should be carefully selected. Other factors, such as interfacial tension and elasticity of the blended polymers, may also influence the blend morphology.

The authors wish to thank the Technology Development Centre of Finland (TEKES) and Neste Foundation for financial support.

REFERENCES

1. J. V. Seppälä, M. T. Heino, and C. Kapanen, *J. Appl. Polym. Sci.*, **44,** 1051 (1992).
2. M. T. Heino and J. V. Seppälä, *J. Appl. Polym. Sci.*, **44,** 2185 (1992).
3. M. T. Heino and J. V. Seppälä, *Polym. Bull.*, **30,** 353 (1993).
4. R. Ramanathan, K. Blizard, and D. Baird, *SPE ANTEC,* **34,** 1123 (1988).
5. D. G. Baird, T. Sun, D. S. Done, and G. L. Wilkes, *J. Thermoplast. Composite Mat.*, **3,** 81 (1990).
6. M. T. Heino and J. V. Seppälä, *J. Appl. Polym. Sci.*, **48,** 1677 (1993).
7. G. I. Taylor, *Proc. R. Soc.*, **A146,** 501 (1934).
8. G. I. Taylor, *Proc. R. Soc.*, **A138,** 41 (1934).
9. S. Wu, *Polym. Eng. Sci.*, **27,** 335 (1987).
10. M. R. Nobile, E. Amendola, L. Nicolais, D. Acierno, and C. Carfagna, *Polym. Eng. Sci.*, **29,** 244 (1989).
11. K. Min, J. L. White, and J. F. Fellers, *Polym. Eng. Sci.*, **24,** 1327 (1987).
12. K. G. Blizard and D. G. Baird, *Polym. News,* **12,** 44 (1986).
13. D. Beery, S. Kenig, and A. Siegmann, *Polym. Eng. Sci.*, **31,** 451 (1991).
14. T. Brinkmann, P. Höck, and W. Michaeli, *SPE ANTEC,* **37,** 988 (1991).
15. D. Done, A. Sukhadia, A. Datta, and D. G. Baird, *SPE ANTEC,* **36,** 1857 (1990).
16. S. Middleman, *Fundamentals of Polymer Processing,* McGraw-Hill, New York, 1977, p. 87.
17. Z. Tadmor and C. G. Gogos, *Principles of Polymer Processing,* Wiley, New York, 1979, p. 425.
18. T. P. Vainio and J. V. Seppälä, *Polymers and Polymer Composites,* accepted for publication, 1993.
19. P. K. H. Heidemeyer, Ph.D. dissertation, Rheinisch-Westfälischen Technischen Hochschule, Aachen (1990).
20. S. Wu, *Polymer Interface and Adhesion,* Marcel Dekker, New York, 1982, p. 102.

Received April 27, 1993
Accepted May 20, 1993

NOMENCLATURE

LCP	Liquid crystalline polymer
PE	Polyethylene
PP	Polypropylene
PS	Polystyrene
SEI	Specific (mechanical) energy input
SEM	Scanning electron microscopy

Symbols

C_L	Centerline distance (of screw axes) (mm)
D	Diameter of the screw or the die (mm)
L	Length of the screw or the die (mm)
$\dot{m}$	Output of the extruder (kg/h)
p	Viscosity ratio = η_{LCP}/η_{PP}
P_{mech}	Mechanical power input of the extruder (kW)
$\dot{Q}$	Volumetric output of the extruder (cm^3/s)
r	Radius of the droplet (μm)
r_{calc}	Radius of the droplet calculated by theory of Wu [Eqs. (3) and (5)] (μm)
R	Radius of the die (cm)
S_0	Cross-sectional area of the die (mm^2)
S_s	Cross-sectional area of the strand (mm^2)
T_m	Melt temperature (°C)
We	Weber number
We_{cr}	Critical Weber number
ϕ	Orientation angle (rad)
$\dot{\gamma}$	Shear rate (s^{-1})
$\dot{\gamma}_{die}$	Shear rate at the die wall (s^{-1})
$\dot{\gamma}_{nozzle}$	Shear rate at the nozzle wall of the injection molding machine (s^{-1})
γ_{12}	Interfacial tension (mN/m)
η	Melt viscosity (Pa)